JOURNAL OF MAGNETIC RESONANCE **132,** 81–87 (1998)
ARTICLE NO. MN981388

Bloch–Siegert Shift Compensated and Cyclic Irradiation Sidebands Eliminated, Double-Adiabatic Homonuclear Decoupling for ^{13}C- and ^{15}N-Double-Labeled Proteins

Shanmin Zhang and David G. Gorenstein

Sealy Center for Structural Biology and the Department of Human Biological Chemistry and Genetics, University of Texas Medical Branch, Galveston, Texas 77555-1157

Received July 7, 1998; revised November 26, 1997

A Gaussian-shaped, offset-independent adiabatic decoupling is adopted to decouple ^{13}CO from $^{13}C_\alpha$ or vice versa for ^{13}C- and ^{15}N-double-labeled proteins, together with a compensating decoupling applied on the opposite side of the $^{13}C_\alpha$ resonance frequency. In a quite broad range, the double-adiabatic decoupling eliminates efficiently the cyclic sidebands caused by direct irradiation of the adiabatic decoupling and reduces significantly the Bloch–Siegert shift. The remaining Bloch–Siegert shift, which is almost a linear function of offset, can be removed by a dilated evolution time. The decoupling sequence is also quite insensitive to the RF field intensity or inhomogeneity due to the reduced transverse components of RF field at $^{13}C_\alpha$, leading to an efficient decoupling even under unfavorable conditions.

INTRODUCTION

In triple-resonance multidimensional NMR, homonuclear ^{13}CO (or $^{13}C_\alpha$) decoupling, during $^{13}C_\alpha$ (or ^{13}CO) evolution time t_1, is often required for ^{13}C- and ^{15}N-double-labeled proteins (*1–3*). It may be accomplished either by a selective 180° refocusing pulse in the middle of the evolution time, or by a selective decoupling pulse, such as the SEDUCE decoupling sequence (*4*), one of the more widely used sequences. Selective refocusing pulses are usually long, which often reduces magnetization due to a T_2 effect. A carefully designed hard 180° pulse may be employed, which rotates ^{13}CO (on-resonance) 180° and at the same time rotates $^{13}C_\alpha$ $n \times 360°$ (off-resonance) using the off-resonance effect, where n is an integer. For $n = 1$, the pulse strength has to satisfy the relationship $f_1 = \Delta f/\sqrt{3}$, where $\Delta f \approx 120$ ppm is the chemical shift difference between the centers of ^{13}CO and $^{13}C_\alpha$ regions. Unfortunately, it requires a high RF field at a high magnetic field. The deviation of the off-resonance rotation becomes larger for larger n. In general, selective refocusing, both for weak and strong pulses, is severely deteriorated by the inhomogeneity of the RF pulse, and by the magnetization leakage due to couplings to other partners. An offset-dependent phase shift will also be introduced due to the ''Bloch–Siegert effect'' (*5–8*). Even though this effect is not induced by the counter-rotating component of the RF field as described in the original discovery (*5*), it is still denoted as the Bloch–Siegert effect, which is, by nature, the offset effect.

SEDUCE decoupling uses a Gaussian-like pulse to replace the rectangular pulse in a phase-modulated broadband decoupling sequence. It reduces the perturbation efficiently outside the decoupling range. The decoupling range per unit RF strength is, however, rather limited; therefore it is not particularly suitable for decoupling in very high magnetic fields, where a broad decoupling range is often necessary.

Adiabatic decoupling (*9–17*) has superb capabilities in terms of the decoupling range as well as the sharp edge of the decoupling profile, mainly because it is quite insensitive to the inhomogeneity of the RF field. It was recently demonstrated by Kupče and Wagner in their homonuclear decoupling with a WURST adiabatic sequence (*15, 16*).

Because of the relative long time period T of an adiabatic inversion compared to the sampling rate, the adiabatic decoupling introduces severe cyclic decoupling sidebands in heteronuclear decoupling, which in turn reduces the intensity of the centerband. The amplitudes of these sidebands can be decreased significantly by increasing the RF decoupling strength and therefore decreasing the decoupling period (*18*), by varying the decoupling period during cycles (*19, 20*), or by phase cycling (*21*). The first method moves the sidebands away from the center; the second one simply spreads out the sidebands; and the third one cancels out the sidebands. Among the three methods, only the first one recovers the intensity loss of the center band. In homonuclear decoupling, ^{13}C–^{13}C decoupling for example, the sidebands are caused mainly by direct irradiation of the decoupling pulse and the cyclic decoupling sidebands are relatively small. The direct irradiation will also introduce a Bloch–Siegert shift that is proportional to the square of the RF strength. Therefore, increasing the RF field strength is not a practical means of reducing homonuclear cyclic irradiation sidebands.

1090-7807/98 $25.00

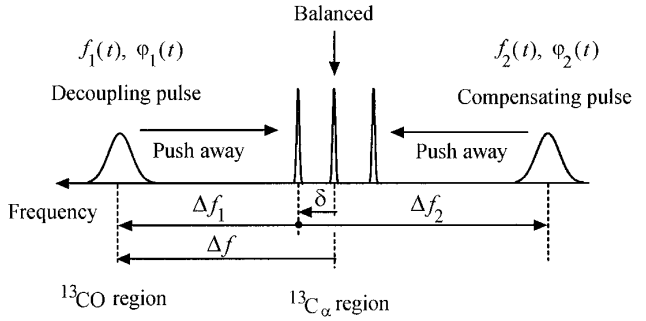

FIG. 1. Adiabatic decouple of ^{13}CO from $^{13}C_\alpha$ with a compensating pulse applied on the other side of the peaks with the same shape but opposite frequency sweep, where $\Delta f = 23.2$ kHz. Both the left and the right peaks are pushed towards the center because of the Bloch–Siegert effect. The center peak is balanced and remains in its position.

As shown by McCoy and Mueller (*7*), the Bloch–Siegert shift can be reduced significantly by using a compensating pulse applied on the other side of the peak. This method, in theory, gets rid of the Bloch–Siegert shift completely only for the center (in the middle of the two decoupling pulses) point. A reduced offset-dependent Bloch–Siegert shift still remains.

An offset-independent adiabatic decoupling (*14, 15, 17*) was used in our $^{13}C_\alpha$–^{13}CO homonuclear decoupling experiments. It has a superb decoupling profile with a quite broad range and a very sharp edge, particularly suitable for homonuclear decoupling. An offset-independent double-adiabatic decoupling with a Gaussian shape is constructed, which removes not only the sidebands but also the remaining Bloch–Siegert shift in a quite broad range with a dilated evolution time.

Similarly to our Double-WURST decoupling (*22*), the double-adiabatic decoupling is constructed with a single waveform generator, but for different purposes. The WURST uses a linear frequency sweep, which gives a quite broad decoupling range but relatively poorer decoupling profile, especially near the edges. Since the Double-WURST was designed for heteronuclear simultaneous decoupling of ^{13}CO and $^{13}C_\alpha$ regions, mainly for reducing RF power, the sharpness of the decoupling profile is not crucial and the Bloch–Siegert shift is totally negligible. The double-adiabatic decoupling uses a nonlinear frequency sweep that is created in such a way that the adiabatic inversion is offset independent (*14, 15, 17*). It leads to a much better decoupling profile, which is important to homonuclear decoupling. The double-adiabatic decoupling can certainly be used in heteronuclear decoupling to replace the Double-WURST.

PRINCIPLES

We consider two arbitrary amplitude- and phase-modulated decoupling sequences with amplitudes $f_1(t)$, $f_2(t)$ and phases $\varphi_1(t)$, $\varphi_2(t)$, respectively, and a period of T ($f_\alpha(nT + t) = f_\alpha(t)$, $\alpha = 1, 2$), as shown in Fig. 1. $f_1(t)$ decouples ^{13}CO from $^{13}C_\alpha$, while $f_2(t)$ is added as a compensating decoupling pulse (*7*). For convenience, the rotating reference frame is chosen at the peak of interest. In this frame both pulses are time dependent, one rotating counterclockwise with a frequency Δf_1 and the other rotating clockwise with a frequency Δf_2.

First, we calculate the interaction acting on the $^{13}C_\alpha$ magnetization caused by the irradiation of only one decoupling field $f_1(t)$. The Hamiltonian for such a system subjected to one phase- and amplitude-modulated RF field can be expressed as (*23, 24*)

$$\begin{aligned} H(t) &= 2\pi f_{1x}(t)[\cos(2\pi\Delta f_1 t)I_x + \sin(2\pi\Delta f_1 t)I_y] \\ &\quad + 2\pi f_{1y}(t)[\cos(2\pi\Delta f_1 t)I_y - \sin(2\pi\Delta f_1 t)I_x] \\ &= 2\pi[f_{1x}(t)\cos(2\pi\Delta f_1 t) - f_{1y}(t)\sin(2\pi\Delta f_1 t)]I_x \\ &\quad + 2\pi[f_{1x}(t)\sin(2\pi\Delta f_1 t) + f_{1y}(t)\cos(2\pi\Delta f_1 t)]I_y, \end{aligned} \quad [1]$$

where $f_{1x}(t) = f_1(t)\cos(\varphi_1(t))$ and $f_{1y}(t) = f_1(t)\sin(\varphi_1(t))$ are the x and y components of the RF fields, respectively. We assume $T = n/\Delta f_1$ (n integer) so that the Hamiltonian is periodic with a period of T. This assumption may cause a percentage error on the order of $1/n$, which is negligible for $n \gg 1$ or $\Delta f_1 T \gg 1$. The zero-order average Hamiltonian is (*25, 26*)

$$\begin{aligned} \bar{H}^{(0)} &= \frac{1}{T}\int_0^T H(t)\,dt \\ &= \frac{2\pi}{T}\int_0^T \{[f_{1x}(t)\cos(2\pi\Delta f_1 t) \\ &\quad - f_{1y}(t)\sin(2\pi\Delta f_1 t)]I_x + [f_{1x}(t)\sin(2\pi\Delta f_1 t) \\ &\quad + f_{1y}(t)\cos(2\pi\Delta f_1 t)]I_y\}\,dt. \end{aligned} \quad [2]$$

It contains four terms, each of which can be calculated using integration by parts. The first term becomes

$$\begin{aligned} &\frac{2\pi I_x}{T}\int_0^T f_{1x}(t)\cos(2\pi\Delta f_1 t)\,dt \\ &= \frac{I_x}{T\Delta f_1}\int_0^T f_{1x}(t)\,d\,\sin(2\pi\Delta f_1 t) \\ &= \frac{I_x}{T\Delta f_1}[f_{1x}(t)\sin(2\pi\Delta f_1 t)|_0^T \\ &\quad - \int_0^T f'_{1x}(t)\sin(2\pi\Delta f_1 t)\,dt] \\ &= \frac{I_x}{2\pi T(\Delta f_1)^2}\int_0^T f'_{1x}(t)\,d\,\cos(2\pi\Delta f_1 t) \end{aligned}$$

$$= \frac{I_x}{2\pi T(\Delta f_1)^2}\,[f'_{1x}(t)\cos(2\pi\Delta f_1 t)|_0^T - \int_0^T f''_{1x}(t)\cos(2\pi\Delta f_1 t)dt]$$

$$= \frac{I_x}{2\pi T(\Delta f_1)^2}\,[(f'_{1x}(T) - f'_{1x}(0)) - \int_0^T f''_{1x}(t)\cos(2\pi\Delta f_1 t)dt], \qquad [3]$$

where integration by parts is used twice, each time a factor Δf_1 is introduced in the denominator. The first term in Eq. [3] is proportional to $1/(\Delta f_1)^2$ denoted as $o(1/(\Delta f_1)^2)$, which approaches zero as $1/(\Delta f_1)^2 \to 0$. The second term can be calculated using integration by parts again, resulting in a higher order term, $o(1/(\Delta f_1)^3)$. For large Δf_1 and small f_1 or $(f_1/\Delta f_1) \ll 1$, Eq. [3] approaches zero. Similarly, one can show that the rest of the terms in Eq. [2] all approach zero on the order of $1/(\Delta f_1)^2$.

The first-order average Hamiltonian has more terms and can be calculated similarly:

$$\begin{aligned}
\bar{H}^{(1)} &= \frac{-i}{2T}\int_0^T dt_2 \int_0^{t_2} [H(t_2), H(t_1)]dt_1 \\
&= \frac{I_z}{2T}\int_0^T 2\pi f_{1x}(t_2)\cos(2\pi\Delta f_1 t_2)dt_2 \\
&\quad\times \int_0^{t_2} 2\pi f_{1y}(t_1)\cos(2\pi\Delta f_1 t_1)dt_1 \\
&\quad- \frac{I_z}{2T}\int_0^T 2\pi f_{1y}(t_2)\cos(2\pi\Delta f_1 t_2)dt_2 \\
&\quad\times \int_0^{t_2} 2\pi f_{1x}(t_1)\cos(2\pi\Delta f_1 t_1)dt_1 \\
&\quad+ \frac{I_z}{2T}\int_0^T 2\pi f_{1x}(t_2)\sin(2\pi\Delta f_1 t_2)dt_2 \\
&\quad\times \int_0^{t_2} 2\pi f_{1y}(t_1)\sin(2\pi\Delta f_1 t_1)dt_1 \\
&\quad- \frac{I_z}{2T}\int_0^T 2\pi f_{1y}(t_2)\sin(2\pi\Delta f_1 t_2)dt_2 \\
&\quad\times \int_0^{t_2} 2\pi f_{1x}(t_1)\sin(2\pi\Delta f_1 t_1)dt_1 \\
&\quad+ \frac{I_z}{2T}\int_0^T 2\pi f_{1x}(t_2)\cos(2\pi\Delta f_1 t_2)dt_2 \\
&\quad\times \int_0^{t_2} 2\pi f_{1x}(t_1)\sin(2\pi\Delta f_1 t_1)dt_1 \\
&\quad- \frac{I_z}{2T}\int_0^T 2\pi f_{1x}(t_2)\sin(2\pi\Delta f_1 t_2)dt_2 \\
&\quad\times \int_0^{t_2} 2\pi f_{1x}(t_1)\cos(2\pi\Delta f_1 t_1)dt_1 \\
&\quad+ \frac{I_z}{2T}\int_0^T 2\pi f_{1y}(t_2)\cos(2\pi\Delta f_1 t_2)dt_2 \\
&\quad\times \int_0^{t_2} 2\pi f_{1y}(t_1)\sin(2\pi\Delta f_1 t_1)dt_1 \\
&\quad- \frac{I_z}{2T}\int_0^T 2\pi f_{1y}(t_2)\sin(2\pi\Delta f_1 t_2)dt_2 \\
&\quad\times \int_0^{t_2} 2\pi f_{1y}(t_1)\cos(2\pi\Delta f_1 t_1)dt_1. \qquad [4]
\end{aligned}$$

There are eight terms in total, and all of them can be calculated using integration by parts. Neglecting all the high-order terms $o(1/(\Delta f_1)^2)$, we find that the first and second terms cancel each other and the third and fourth terms cancel each other as well. As an example, the fifth term can be calculated as

$$\begin{aligned}
&\frac{I_z}{2T}\int_0^T 2\pi f_{1x}(t_2)\cos(2\pi\Delta f_1 t_2)dt_2 \\
&\quad\times \int_0^{t_2} 2\pi f_{1x}(t_1)\sin(2\pi\Delta f_1 t_1)dt_1 \\
&= -\frac{I_z}{2T2\pi\Delta f_1}\int_0^T 2\pi f_{1x}(t_2)\cos(2\pi\Delta f_1 t_2)dt_2 \\
&\quad\times \int_0^{t_2} 2\pi f_{1x}(t_1)d\,\cos(2\pi\Delta f_1 t_1) \\
&\approx -\frac{I_z}{2T\Delta f_1}\int_0^T 2\pi f_{1x}^2(t_2)\cos^2(2\pi\Delta f_1 t_2)dt_2. \qquad [5]
\end{aligned}$$

The other terms can be calculated in a similar way. The first-order average Hamiltonian is then the sum of all the remaining terms,

$$\begin{aligned}
\bar{H}^{(1)} \approx &-\frac{I_z}{2T\Delta f_1}\int_0^T 2\pi f_{1x}^2(t_2)\cos^2(2\pi\Delta f_1 t_2)dt_2 \\
&-\frac{I_z}{2T\Delta f_1}\int_0^T 2\pi f_{1x}^2(t_2)\sin^2(2\pi\Delta f_1 t_2)dt_2 \\
&-\frac{I_z}{2T\Delta f_1}\int_0^T 2\pi f_{1y}^2(t_2)\cos^2(2\pi\Delta f_1 t_2)dt_2 \\
&-\frac{I_z}{2T\Delta f_1}\int_0^T 2\pi f_{1y}^2(t_2)\sin^2(2\pi\Delta f_1 t_2)dt_2
\end{aligned}$$

$$= -\frac{I_z}{2T\Delta f_1}\int_0^T 2\pi[f_{1x}^2(t_2) + f_{1y}^2(t_2)]dt_2$$
$$-\frac{2\pi I_z}{2\Delta f_1}\left[\int_0^T f_1^2(t_2)dt_2/T\right]$$
$$= -\frac{2\pi f_{1rms}^2}{2\Delta f_1} I_z \text{ (in rad)}$$
$$= -\frac{f_{1rms}^2}{2\Delta f_1} I_z \text{ (in Hz)}, \quad [6]$$

where f_{1rms} stands for the root-mean-square value of $f_1(t)$ defined as $f_{1rms} = (1/\sqrt{T})\sqrt{\int_0^T f_1^2(t)dt}$. Even though it is derived differently, Eq. [6] is the same as that obtained by Warren (*27*) in calculating far off-resonance excitation. A similar result was obtained by Emsley and Bodenhausen (*28*). The negative sign of the Bloch–Siegert shift ensures that the shift has a repulsive nature, i.e., the peak is always pushed away from the pulse as shown in Fig. 1.

Now, the Bloch–Siegert shift caused by the second decoupling pulse can be added. The shift produced by the double-decoupling pulse is simply the sum of two terms (Eq. [6]) if the two pulses are far away from each other and therefore there is no interference between them,

$$H^{(1)} \approx \left[-\frac{f_{1rms}^2}{2\Delta f_1} - \frac{f_{2rms}^2}{2\Delta f_2}\right] I_z, \quad [7]$$

where Δf_2 (= peak frequency − decoupling frequency) is negative (Fig. 1). In the case of $f_{1rms}^2 = f_{2rms}^2$, Eq. [7] becomes

$$H^{(1)} \approx -f_{1rms}^2\left[\frac{1}{2\Delta f_1} + \frac{1}{2\Delta f_2}\right] I_z$$
$$\approx -\frac{f_{1rms}^2}{2}\left(\frac{2\delta}{\Delta f^2 - \delta^2}\right) I_z$$
$$\approx -\frac{f_{1rms}^2}{2\Delta f}\left(\frac{2\delta}{\Delta f}\right) I_z, \quad [8]$$

where $\Delta f = (\Delta f_1 + |\Delta f_2|)/2$ is the frequency difference from the center of the two decoupling pulses to the left pulse and δ is the offset of peak measured from the same center as shown in Fig. 1.

Equation [8] shows that the Bloch–Siegert shift is scaled by a factor of $(2\delta/\Delta f)$ for the double decoupling. For $\delta = 0$, the Bloch–Siegert shift vanishes; for $\delta > 0$, the shift is negative; and for $\delta < 0$, the shift is positive. The whole spectrum is therefore contracted by a factor of (Eq. [8])

$$\lambda = [1 - (f_{1rms}/\Delta f)^2], \quad [9]$$

substantially reducing the Bloch–Siegert shift. To compensate for the remaining effect, a dilated evolution time,

$$t_1' = \frac{t_1}{\lambda} \approx [1 + (f_{1rms}/\Delta f)^2]t_1, \quad [10]$$

can be used in the experiment, leading to a spectrum without any Bloch–Siegert shift in a quite broad range (Fig. 5).

If $f_2(t) = f_1(t)$ and $\varphi_2(t) = -\varphi_1(t)$, corresponding to a same amplitude but opposite frequency sweep of the adiabatic decoupling, the Hamiltonian for the two decoupling RF fields becomes (for $\delta = 0$)

$$H(t) = 4\pi f_1(t)\cos[2\pi\Delta f t + \varphi(t)]I_x. \quad [11]$$

Importantly, in this Hamiltonian, the I_y component disappears and the RF field is no longer phase modulated. The amplitude $f_1(t)$ is now modulated by $\cos[2\pi\Delta f t + \varphi(t)]$. As a result, the sidebands located at n/T disappear, and all the higher-order average Hamiltonians vanish because $[H(t'), H(t'')] = 0$ (for arbitrary t' and t'') even at high RF amplitudes. Under off-resonance condition, $\delta \neq 0$ and $[H(t'), H(t'')] \neq 0$, high-order average Hamiltonians remain as a function of δ.

To understand the cyclic sidebands caused by periodic irradiation of the decoupling pulse $f_1(t)$ of period T, we introduce a time-dependent $f_{1rms}(t)$ defined as

$$f_{1rms}^2(t) = \frac{1}{t}\int_0^t f_1^2(t')dt'. \quad [12]$$

The first-order average Hamiltonian at time t becomes

$$H^{(1)}(t) = -\frac{f_{1rms}^2(t)}{2\Delta f_1} I_z = -\left[\frac{f_{1rms}^2(t) - f_{1rms}^2}{2\Delta f_1} I_z\right]$$
$$-\frac{f_{1rms}^2}{2\Delta f_1} I_z$$
$$= H(t) - \frac{f_{1rms}^2}{2\Delta f_1} I_z. \quad [13]$$

The second term simply gives a Bloch–Siegert shift. The first term, $H(t)$, is periodic with a period of T and $H(nT) = 0$. Since $H(t)$ commutes with the second term, it acts independently on the initial density matrix and causes a periodic modulation of the FID, which in turn produces sidebands after Fourier transformation. The modulation term $H(t)$ (Eq. [13]) changes sign when the decoupling pulse moves from the left side of the peak to the right side (Fig. 1). Consequently, the sign of modulation of the sidebands

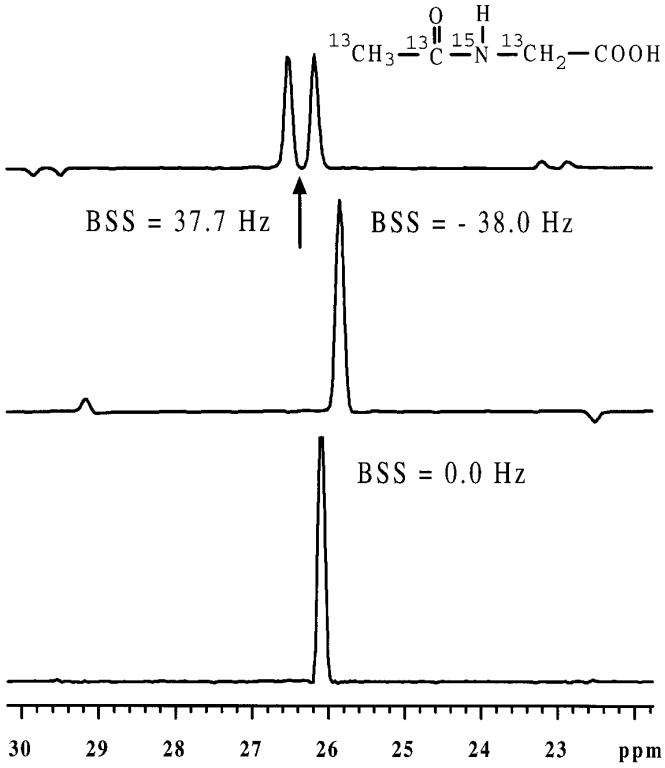

FIG. 2. $^{13}CH_3$ spectra obtained from the traces of two-dimensional HSQC spectra using a test sample of *N*-acetylglycine. The spectra are acquired with a single adiabatic decoupling (middle), with a compensating decoupling (top), and with a double-adiabatic decoupling (bottom), where BSS stands for the Bloch–Siegert shift. The decouple pulse has a Gaussian shape, $A(t) = f_{1max}\exp[-\alpha(t - T/2)^2]$ (α = 5 (kHz)^2, T = 2 ms, f_{1max} = 2.50 kHz, and f_{1rms} = 1.32 kHz), a phase cycle of (0°, 150°, 60°, 150°, 0°), and a frequency sweep of 8 kHz.

changes (Fig. 2). Thus, in accordance with the previous argument, the sidebands can be balanced with two decoupling pulses of the same amplitude-modulation but the opposite location and opposite frequency sweep.

EXPERIMENTAL

To get a sharp decoupling range we used an offset-independent adiabatic decoupling (*14, 15, 17*) with a Gaussian shape, $A(t) = f_{1max}\exp[-\alpha(t - T/2)^2]$ (α = 2.55 (kHz)^2, T = 2.8 ms), and a phase cycle of (0°, 150°, 60°, 150°, 0°) (*29, 30*) (except for experiments in Fig. 2). The pulse has a maximum RF field strength of f_{1max} = 2.38 kHz and a root-mean-square value of f_{1rms} = 1.26 kHz. The frequency sweep is nonlinear and is constructed according to reference (*14*). The total sweep is 8 kHz, which gives almost the same decoupling range.

To test ^{13}C homonuclear decoupling, a HMQC (*31*) sequence (except for experiments in Fig. 2) with water suppression was used with a test sample of ^{15}N- and ^{13}C-labeled (-COOH is unlabeled) *N*-acetylglycine. The ^{13}C carrier frequency is applied at the methyl $^{13}CH_3$ at 26.07 ppm. A frequency-shifted decoupling is applied to ^{13}CO (*22, 32*), with a phase increment of $\Delta\varphi$ = 23.4° and time increment of Δt = 2.8 μs, corresponding to a frequency shift of 23.2 kHz. A compensating decoupling sequence is applied at −23.2 kHz with the same RF amplitude modulation but opposite frequency sweep. All the experiment were performed on a Varian Unity-Plus 600-MHz instrument using a 5 mm HCN triple-resonance probe.

Figure 2 shows the ^{13}C spectra of *N*-acetylglycine obtained from the traces of the indirectly detected dimension of HSQC. The middle spectrum is obtained with a single adiabatic decoupling $f_1(t)$ (Fig. 1), which causes a Bloch–Siegert shift of −38.0 Hz and cyclic irradiation sidebands at $\pm 1/T$ (opposite phase) from the center peak (*15*). Unlike the heteronuclear decoupling, where the sidebands are introduced by the modulation of heteronuclear coupling by the decoupling pulse and one usually sees the same phase for all the sidebands, the ^{13}C homonuclear cyclic sidebands, in our case, are introduced by direct irradiation of the decoupling pulse. The intensities and phases of these sidebands are therefore determined by the decoupling amplitude and phase modulations. As in the heteronuclear decoupling, the pulse also causes a modulation of homonuclear coupling, which, in theory, will also cause homonuclear cyclic decoupling sidebands. These sidebands, however, are negligibly small in our experiments because of the smaller $^{13}C-^{13}C$ homonuclear coupling, and they cannot be removed by the compensating pulse.

The spectrum at the top of Fig. 2 is obtained with the compensating decoupling pulse. Since it is located 46 kHz away from the ^{13}CO, there is no decoupling effect and the $^{13}CH_3$ peak is split in two with a separation of the $^{13}CO-^{13}CH_3$ J coupling constant. Also, because the compensating pulse is applied on the other side of the peak, which changes the sign of the Bloch–Siegert term (Eq. [7]) or the sign of the modulation of the FID, the peaks are shifted to the left side almost the same amount and the spectrum has negative sidebands relative to the middle spectrum, as expected.

The spectrum at the bottom of Fig. 2 is obtained with the double-adiabatic decoupling pulse, one located at −23.2 kHz and the other at 23.2 kHz. To use the double decoupling the RF power level has to be increased 6 dB, which corresponds to double the amplitude. The f_{1rms} and the RF power, however, have been increased only by factors of $\sqrt{2}$ and 2, respectively, because of the interference of the two decoupling pulses. The Bloch–Siegert shift and sidebands are balanced by the compensating pulse. Also, the amplitude is higher than that of the middle one.

Similar results were obtained for ^{13}C off-resonance δ ranging from −3 to 3 kHz, where $|\delta|/\Delta f < 0.13$ can be treated as close to on-resonance.

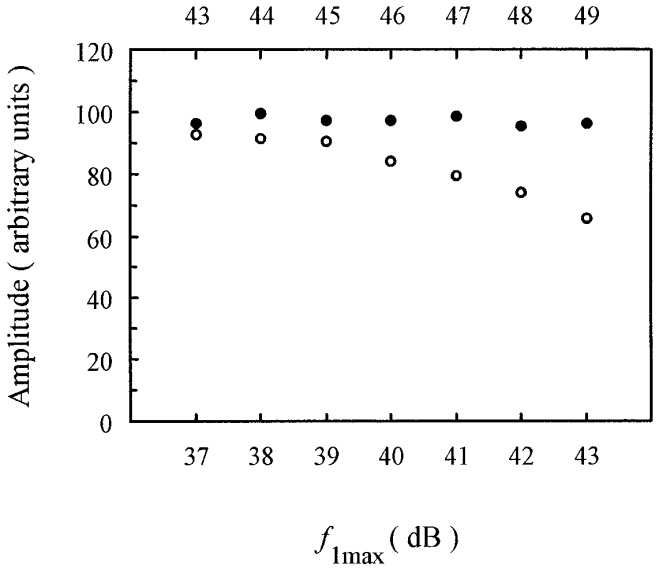

FIG. 3. Amplitude versus RF field strength for single- (open circles) and double-adiabatic (filled circles) decouplings, where 40 dB corresponds to a RF field f_{1max} = 2.37 kHz or f_{1rms} = 1.26 kHz. For double-adiabatic decoupling, the RF field strength is shown on the top and is increased 6 dB, accordingly.

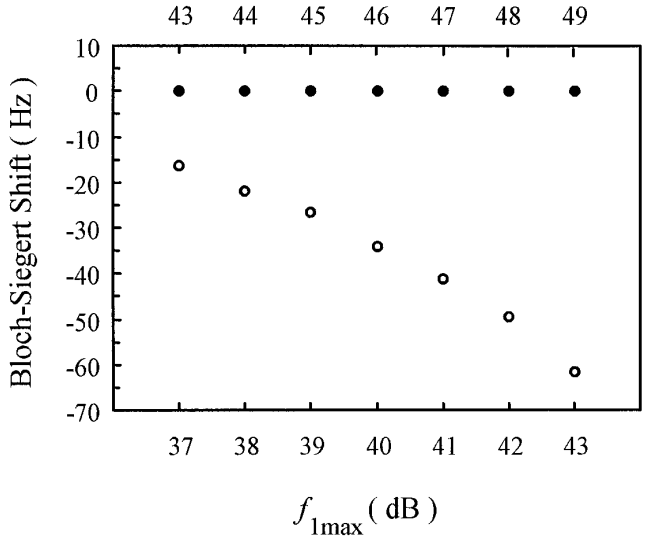

FIG. 4. Bloch–Siegert shift versus RF field strength for single- (open circles) and double-adiabatic (filled circles) decouplings for offset $\delta = 0$, where 40 dB corresponds to a RF field f_{1max} = 2.37 kHz or f_{1rms} = 1.26 kHz. For double-adiabatic decoupling, the RF field strength is shown on the top and is increased 6 dB, accordingly.

Figure 3 shows the peak amplitudes versus the pulse strength. For single-adiabatic decoupling, the amplitude decreases as the pulse strength increases (open circles). This behavior is expected, since the high-order average Hamiltonians contribute at high pulse strength and they include I_x and I_y terms that partially destroy the magnetization. For double-adiabatic decoupling, however, all the high-order average Hamiltonians vanish because of the commuting properties, as discussed earlier. As a consequence, the amplitude is almost independent of the pulse strength. This is only true for peaks exactly on resonance ($\delta = 0$). For off-resonance peaks, the amplitudes will change slightly.

As shown in Eq. [6], the Bloch–Siegert shift depends on the *rms* value of the RF pulse strength for single decoupling. For double decoupling, however, the Bloch–Siegert shift is balanced, resulting in a pulse-strength-independent shift as demonstrated in Fig. 4. Again, this is only for an on-resonance condition ($\delta = 0$).

According to Eqs. [6] and [8], both single and double decoupling will introduce offset-dependent Bloch–Siegert shifts. The double decoupling reduces the Bloch–Siegert shift significantly and makes the shift antisymmetrical with zero shift at on-resonance, which corresponds to scaling the spectrum or pushing the peaks to the center by the double-decoupling sequence (Fig. 1). The scaled spectrum can be easily corrected by a dilated evolution time t_1 (Eq. [10]), as shown experimentally in Fig. 5.

CONCLUSIONS

Unlike heteronuclear decoupling, the cyclic sidebands for $^{13}C-^{13}C$ homonuclear decoupling are caused mainly by direct irradiation of the decoupling fields rather than by the modulation of the J coupling. The phase and amplitude are therefore determined by the pulse shape, strength, and location. The cyclic irradiation sidebands change sign when the decoupling pulse moves from left side of the peak to the right side, which makes cancellation of the sidebands possible by a compensating decoupling pulse with the same shape but opposite location and sweep. The small offset-dependent

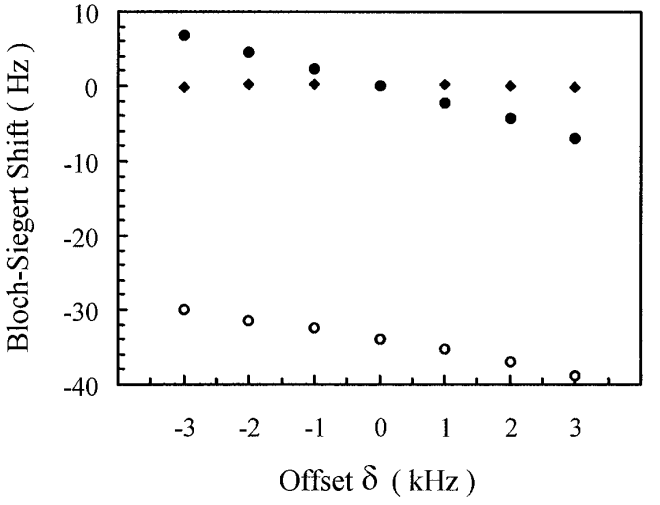

FIG. 5. Bloch–Siegert shift versus offset δ for single- (open circles) and double-adiabatic (filled circles) decouplings, as well as for double-adiabatic decoupling with a dilated evolution time $1.00223t_1$ (filled diamonds).

Bloch–Siegert shift for a double decoupling can be removed in a quite broad range by a dilated evolution time. The double-adiabatic decoupling is less sensitive to the pulse strength and therefore to the inhomogeneity of RF field, leading to a homonuclear decoupling superior to the single-adiabatic decoupling. The double-adiabatic decoupling can be easily generated with a single waveform generator and is easily implemented in all the triple-resonance multidimensional pulse sequences for ^{13}C- and ^{15}N-double-labeled proteins. Also, the double-adiabatic decoupling can be used interchangeably in HNCA and HNCO experiments, where the compensating pulse and decoupling pulse change their roles. Therefore, these two pulse sequences can be combined to one.

ACKNOWLEDGMENTS

This research was supported by NIH (AI27744), NIEHS (ES06676), the Welch Foundation (H-1296), the Lucille P. Markey Foundation, and the Sealy and Smith Foundation. Building funds were provided by NIH (1CO6CA59098).

REFERENCES

1. L. E. Kay, M. Ikura, R. Tschudin, and A. Bax, *J. Magn. Reson.* **89,** 496 (1990).
2. D. R. Muhandiram and L. E. Kay, *J. Magn. Reson. B* **103,** 203 (1994).
3. L. E. Kay, G. Y. Xu, and T. Yamazaki, *J. Magn. Reson. A* **109,** 129 (1994).
4. M. A. McCoy and L. Mueller, *J. Am. Chem. Soc.* **114,** 2108 (1992).
5. F. Bloch and A. Siegert, *Phys. Rev.* **57,** 552 (1940).
6. S. Grzesiek and A. Bax, *J. Magn. Reson.* **96,** 432 (1992).
7. M. A. McCoy and L. Mueller, *J. Magn. Reson.* **98,** 674 (1992).
8. G. W. Vuister and A. Bax, *J. Magn. Reson.* **98,** 428 (1992).
9. M. S. Silver, R. I. Joseph, C.-N. Chen, V. J. Sank, and D. I. Hoult, *Nature* **310,** 681 (1984).
10. J. Baum, R. Tyko, and A. Pines, *Phys. Rev. A* **32,** 3435 (1985).
11. M. R. Bendall, *J. Magn. Reson. A* **112,** 126 (1995).
12. Ē. Kupče and R. Freeman, *J. Magn. Reson. A* **115,** 273 (1995).
13. R. Fu and G. Bodenhausen, *J. Magn. Reson. A* **117,** 324 (1995).
14. A. Tannús and M. Garwood, *J. Magn. Reson. A* **120,** 133 (1996).
15. Ē. Kupče and G. Wagner, *J. Magn. Reson. B* **109,** 329 (1995).
16. H. Matsuo, Ē. Kupče, H. Li, and G. Wagner, *J. Magn. Reson. B* **113,** 91 (1995).
17. Ē. Kupče and R. Freeman, *J. Magn. Reson. A* **118,** 299 (1996).
18. Ē. Kupče and R. Freeman, *J. Magn. Reson. A* **117,** 246 (1995).
19. A. J. Shaka, P. B. Barker, C. J. Bauer, and R. Freeman, *J. Magn. Reson.* **65,** 535 (1985).
20. T. Hwang, M. Garwood, A. Tannus, and P. C. M. van Zijl, *J. Magn. Reson. A* **121,** 221 (1996).
21. Ē. Kupče and R. Freeman, ENC, Orlando, 1997.
22. S. Zhang, J. Wu, and D. G. Gorenstein, *J. Magn. Reson. A* **123,** 181 (1996).
23. A. Abragam, ''Principle of Nuclear Magnetism,'' Oxford Univ. Press, Oxford (1961).
24. R. R. Ernst, G. Bodenhausen, and A. Wokaun, ''Principles of Nuclear Magnetic Resonance in One and Two Dimensions,'' Clarendon, Oxford (1987).
25. U. Haeberlen and J. S. Waugh, *Phys. Rev.* **175,** 453 (1968).
26. M. Mehring, ''High Resolution NMR Spectroscopy in Solids,'' Springer, Berlin (1976).
27. W. S. Warren, *J. Chem. Phys.* **81,** 5437 (1984).
28. L. Emsley and G. Bodenhausen, *Chem. Phys. Lett.* **168,** 297 (1990).
29. R. Tycko, A. Pines, and R. Gluckenheimer, *J. Chem. Phys.* **83,** 2775 (1985).
30. T. Fujiwara and K. Nagayama, *J. Magn. Reson.* **77,** 53 (1988).
31. M. F. Summers, L. G. Marzilli, and A. Bax, *J. Am. Chem. Soc.* **108,** 4285 (1986).
32. S. Zhang and D. G. Gorenstein, *J. Chem. Phys.* **105,** 5659 (1996).